[16] J. Lothe, J. Appl. Phys. 31, 1077 (1960).

[17] J. Friedel, *Dislocations* (Pergamon, New York, 1964), Chap. V.

[18] R. M. Thomson and R. W. Balluffi, J. Appl. Phys. 33, 803 (1962); 33, 817 (1962).

[19] See, for example, E. S. Wajda *et al.*, Acta Met. 3, 39 (1955); J. S. Warford and H. B. Huntington, Phys. Rev. B 1, 1867 (1970).

[20] R. W. Balluffi and D. N. Seidman, J. Appl. Phys. 36, 2708 (1965).

[21] D. N. Seidman and R. W. Balluffi, Phys. Status Solidi 17, 531 (1966).

PHYSICAL REVIEW B VOLUME 5, NUMBER 4 15 FEBRUARY 1972

Dilatometric and X-Ray Thermal Expansion in Noncubic Crystals. II. Experiments on Cadmium†

R. Feder
IBM Watson Research Center, Yorktown Heights, New York 10598

and

A. S. Nowick
Henry Krumb School of Mines, Columbia University, New York, New York 10027

(Received 22 September 1971)

Precision measurements of macroscopic thermal expansion $\delta l/l_0$ and microscopic (x-ray) thermal expansion $\delta d/d_0$ have been carried out for cadmium single crystals in both the a and c directions, between room temperature and the melting point. In accordance with the prediction of the previous paper (paper I) it was found that the difference $\Delta = (\delta L/L_0) - (\delta d/d_0)$ in a given direction is sample dependent. Accordingly, information on the equilibrium defect concentration was obtained from samples cut from the same large crystal. The mole fraction of vacancies in equilibrium, given by $2\Delta_a + \Delta_c$, has the value 5.6×10^{-4} at the melting point. The results as a function of temperature are consistent with an interpretation in terms of monovacancies only, with enthalpy and entropy of formation, respectively, of (0.40 ± 0.02) eV and $(0.3\pm0.4)\,k$. With the aid of self-diffusion data, appropriate vacancy-migration parameters are also obtained. In addition, the ratio Δ_c/Δ_a is found to be independent of temperature, and is interpreted in accordance with the theory of paper I. In particular, it is found that nonbasal dislocations play a large role as sources and sinks for vacancies.

I. INTRODUCTION

The previous paper[1] (henceforth called paper I) discusses the theory involved in the comparison of precision dilatometric and x-ray thermal-expansion measurements at high temperatures for axial crystals. It is shown that if vacancies are the predominant defects present in thermal equilibrium at temperatures near the melting point, the vacancy concentration is given by

$$\overline{C}_v(T) = 2\Delta_a(T) + \Delta_c(T)\ , \tag{1}$$

where $\Delta \equiv (\delta L/L_0) - (\delta d/d_0)$ is the difference between the macroscopic and microscopic expansions between the reference temperature T_0 and an elevated temperature T. The quantity $\overline{C}_v(T)$ is a thermodynamic quantity and, therefore, should be independent of the sample studied. On the other hand, it is pointed out that the separate quantities Δ_a and Δ_c may be sample dependent. The major emphasis of paper I is on the interpretation of the ratio Δ_c/Δ_a in terms of the parameters of dislocation climb.

Equation (1) gives the total number of vacant lattice sites regardless of whether or not vacancies are combined into higher clusters (divacancies, trivacancies, etc.). If, however, primarily monovacancies are present (as has usually been the case for cubic crystals[2]), $\overline{C}_v(T)$ is given by

$$\overline{C}_v(T) = A\, e^{-H_v^f/kT}\ , \tag{2}$$

with

$$A = e^{S_v^f/k}\ , \tag{3}$$

in which H_v^f and S_v^f are, respectively, the enthalpy and entropy of formation of a vacancy. These two parameters may then be obtained, in the usual way, from the slope and intercept, respectively, of a plot of $\ln\overline{C}_v$ vs T^{-1}.

The present paper is concerned with describing measurements of $\Delta_a(T)$ and $\Delta_c(T)$ for metallic cadmium, in order to obtain the quantities H_v^f and S_v^f, as well as to examine the ratio Δ_c/Δ_a in terms of the dislocation-climb theory presented in paper I. In view of the indication in that paper of possible sample dependence of Δ_a and Δ_c, we have carried out the principal measurements on samples cut from one large single crystal. In addition, however, data were taken on several other crystals to see if the predicted sample dependence does, in fact, occur. The results are then compared with those reported recently for other hexagonal metals

TABLE I. Specimens used in the dilatometer.

Specimen	θ[a]	Origin
A_{18}	18°	Bridgman grown
B_c	0°	Cut from boule[b]
B_a	90°	Cut from boule
B_{18}	18°	Cut from boule
E_{85}	85°	Bridgman grown
S_c	0°	Seeded, horizontal boat

[a] θ is the angle between the specimen axis and the c axis.
[b] The boule itself was Bridgman grown.

(Zn[3] and Mg[4]).

II. EXPERIMENTAL METHODS

A. Specimen Preparation

Most of the single crystals used were grown by the Bridgman method from high-purity (99.999%) cadmium in graphite crucibles which were sealed inside evacuated quartz tubes. The Bridgman crystals were 1 cm in diameter, except for a large crystal grown in a 3-cm-diam crucible. One crystal was grown by a seeding technique in which a seed, cut from a Bridgman-grown crystal, was oriented in a horizontal alumina boat containing cadmium metal, with the c axis parallel to the long axis of the boat. The seed was used to initiate the growth of a single crystal by passing a single hot zone from the middle of the seed to the other end of the boat. This crystal was therefore hemispherical in cross section and about 1.2 cm in diameter.

The various single crystals were individually mounted on a goniometer table and glued to the table with a low-temperature cement. The 1-cm-diam Bridgman-grown crystals were mounted with the goniometer table on a spark cutter, modified so that two wire blades, 5 cm apart, were arranged to cut simultaneously. Once the crystal was aligned such that its long axis was perpendicular to the wire blades, a single cut produced a 5-cm-long cylindrical specimen with faces parallel to each other and perpendicular to the long axis. The seeded crystal was mounted and cut on the spark cutter in a similar fashion. The 3-cm-diam Bridgman crystal, which will be referred to as the large crystal or "boule," was oriented using x rays and found to have its growth axis at 37° to the c axis. With a single wire blade, three samples were spark cut from this boule having the long axis parallel to the c axis, perpendicular to the c axis, and at 18° to the c axis, respectively. Further, cuts were made on these samples so that each had a 1-cm-square cross section and a length of about 3 cm. The end surfaces of all specimens used for the dilatometric measurements were made parallel to each other within several wavelengths of light by holding them in a precision ground "V" block and polishing with a compound on an optical flat. A listing of all of the dilatometric samples is given in Table I.

Samples for the x-ray measurements were obtained from the 1- and 3-cm Bridgman-grown crystals. The crystals were oriented by taking x-ray Laue patterns. Some specimens were spark cut with faces parallel to the basal (0001) plane, while others were cut parallel to the $(10\bar{1}0)$ plane. The final specimens were in the form of 3-mm-thick wafers.

All specimens cut for both the length measurements and the x-ray measurements were etched in a dilute solution of nitric acid to remove the cold work left by the spark cutting and the polishing. X-ray Laue patterns were then employed to determine if the cold-worked layer had been completely removed.

B. X-Ray Method

The x-ray equipment used to measure the lattice parameter as a function of temperature is similar to that described in previous work.[5] A calibrated chromel-alumel thermocouple was imbedded in the specimen holder to prevent contamination by the cadmium vapor. The end of the thermocouple was approximately 1 mm from the specimen. Helium gas at a pressure of 100 Torr was used as an exchange gas to minimize temperature gradients in the specimen chamber. To determine the lattice constant a, x-ray measurements on the $(10\bar{1}0)$-oriented wafers were made of the $30\bar{3}0$ reflection using Ni$K\alpha_1$ radiation. For the lattice constant c, the (0001)-oriented wafers and the 0006 reflection were utilized, with Co$K\alpha_1$ radiation. Over the temperature range from 0 to 319 °C the Bragg angle which gave the lattice constant a varied from 75° to 72.5°, while the corresponding Bragg angle for the lattice constant c varied from 73° to 70°. The precision of measurement of both lattice constants was 10 to 12 ppm.

C. Dilatometric Method

Lengths were measured using a Fizeau-type interferometer similar to that described previously.[5] The specimen in the present case was in the form of a rod having a circular or square cross section. The optical flats were placed over the upper and lower ground surfaces of the specimen but off center, so as to create a gap alongside of the specimen for the appearance of interference fringes. A calibrated chromel-alumel thermocouple was used to indicate the temperature. It was inserted into a thin nickel tube which acted as a sheath to prevent contamination by the cadmium vapor. The precision of the dilatometric measurements for a 5-cm-diam specimen was approximately 1 ppm.

III. CORRECTION OF DATA FOR OFF-AXIS SAMPLES

Although, theoretically, the only required expansions are those parallel and perpendiuclar to the c axis, some of the crystals used in the dilatometric measurements were oriented at an arbitrary angle θ with respect to the c axis. It is therefore necessary to convert the expansion $(\delta L/L_0)_\theta$ of such a crystal into the quantities of interest, $(\delta L/L_0)_c$ and $(\delta L/L_0)_a$. If the total expansion $(\delta L/L_0)_\theta$ is small, it can be treated as a component of strain (i.e., of a second-rank symmetric tensor) to give the relation

$$(\delta L/L_0)_\theta = (\delta L/L_0)_c \cos^2\theta + (\delta L/L_0)_a \sin^2\theta \ . \tag{4}$$

Thus, from measurements on two off-axis samples, one can obtain both $(\delta L/L_0)_a$ and $(\delta L/L_0)_c$. In view of concern over possible sample dependences of the thermal expansions, we have used a modified procedure, taking only samples for which θ is either relatively small, or else close to 90°. In the case of small θ, we used Eq. (4) to obtain $(\delta L/L_0)_c$, treating the term in $(\delta L/L_0)_a$ as a correction term. Thus,

$$(\delta L/L_0)_c = (\delta L/L_0)_\theta \sec^2\theta + (\delta L/L_0)_a \tan^2\theta \ . \tag{5}$$

If the last term is relatively small, $(\delta L/L_0)_a$ may be taken from data on a sample cut from the large boule and oriented in the basal plane; or it may even be replaced by $\delta a/a_0$, as measured by x rays, since the contribution due to vacancies will be of negligible importance in this small correction term. Similarly, for θ close to 90°, $(\delta L/L_0)_a$ may be obtained from the data for $(\delta L/L_0)_\theta$ using $(\delta L/L_0)_c$ in the small correction term.

Since the strains $\delta L/L_0$ attain values as large as 1%, we must consider whether Eq. (4) is suitable. An exact relation[4] is readily obtained from the Pythagorean theorem, or in more convenient form, one may expand to obtain a second-order term $\frac{1}{2}\cos^2\theta \sin^2\theta \, [(\delta L/L_0)_c - (\delta L/L_0)_a]^2$ which should be added to the right-hand side of Eq. (4). For the θ values used here, this term amounts to just below 1×10^{-5} and is therefore negligible, within experimental error.

Finally, we have considered a correction for the shearing of an off-axis specimen with change in the temperature, since the dilatometer measures, not δL, but $\delta(L\cos\alpha)$, where α is the shear angle. However, this correction turns out to be well below 1×10^{-5} for the present samples.

IV. RESULTS

All thermal-expansion measurements, both x ray and dilatometric, showed complete reversibility with respect to temperature cycling. The data to be presented will, therefore, not distinguish points taken during heating and during cooling, although considerable cycling was actually carried out.

Data from expansion parallel to the c axis are shown in Fig. 1. This figure presents the fractional length change $(\delta L/L_0)_c$ and the fractional change in lattice constant $\delta c/c_0$ as a function of temperature, where the starting temperature, denoted by subscript zero, is 20 °C, and measurements are made almost up to the melting point 320.9 °C. The x-ray points are denoted by ×'s while the dilatometric data shown are from three different samples: B_c, A_{18}, and S_c (see Table I). Since B_c and S_c are oriented parallel to the c axis, the data from these two samples are plotted directly as measured. The data for sample A_{18}, for which $\theta = 18°$, were not plotted directly but were corrected with the aid of Eq. (5) and the data (to be presented below) for a crystal oriented in the basal plane. The correction term in Eq. (5) is only about 10% of the main term, so that the choice of which crystal to use for the $(\delta L/L_0)_a$ data is unimportant, as already mentioned below Eq. (5). All of the data shown in Fig. 1, both x ray and dilatometric, are coincident up to about 165 °C, to within experimental error. Above this temperature, the macroscopic-expansion data begin to diverge from the x-ray data. However, the data from sample A_{18} diverge more slowly than that from the other two samples, and reach only about half the separation from the x-ray data attained by the other samples just below 320 °C. On the other hand the data for the seeded crystal S_c and the one cut from the boule B_c are in close agreement over the entire temperature range.

In a similar fashion, data for thermal expansion in the basal plane are presented in Fig. 2. The x-ray data are again represented by the symbol ×, while the dilatometric data are from samples B_a, cut from the boule, and E_{85}, where the latter is corrected to $(\delta L/L_0)_a$ with the aid of Eq. (4) and the data for $(\delta L/L_0)_c$ already given. Because θ is so close to 90° for this latter sample, the correction term is very small. Again, all of the data are coincident in the lower temperature range, up to about 180 °C, above which the dilatometric data begin to diverge from the x-ray data. This time, the divergence of data for sample E_{85} is greater than that for sample B_a, as shown by the dashed upper curve.

The x-ray data in Figs 1 and 2 were obtained in each case from three different specimens. These figures show that there are no discrepancies in the results from the different specimens. The absolute values of the lattice parameters at 26 °C, obtained in this work by averaging over the various specimens, and their comparison with the ASTM values,[6] are given in Table II. Table III presents the present values of the expansions $\delta a/a_0$ and

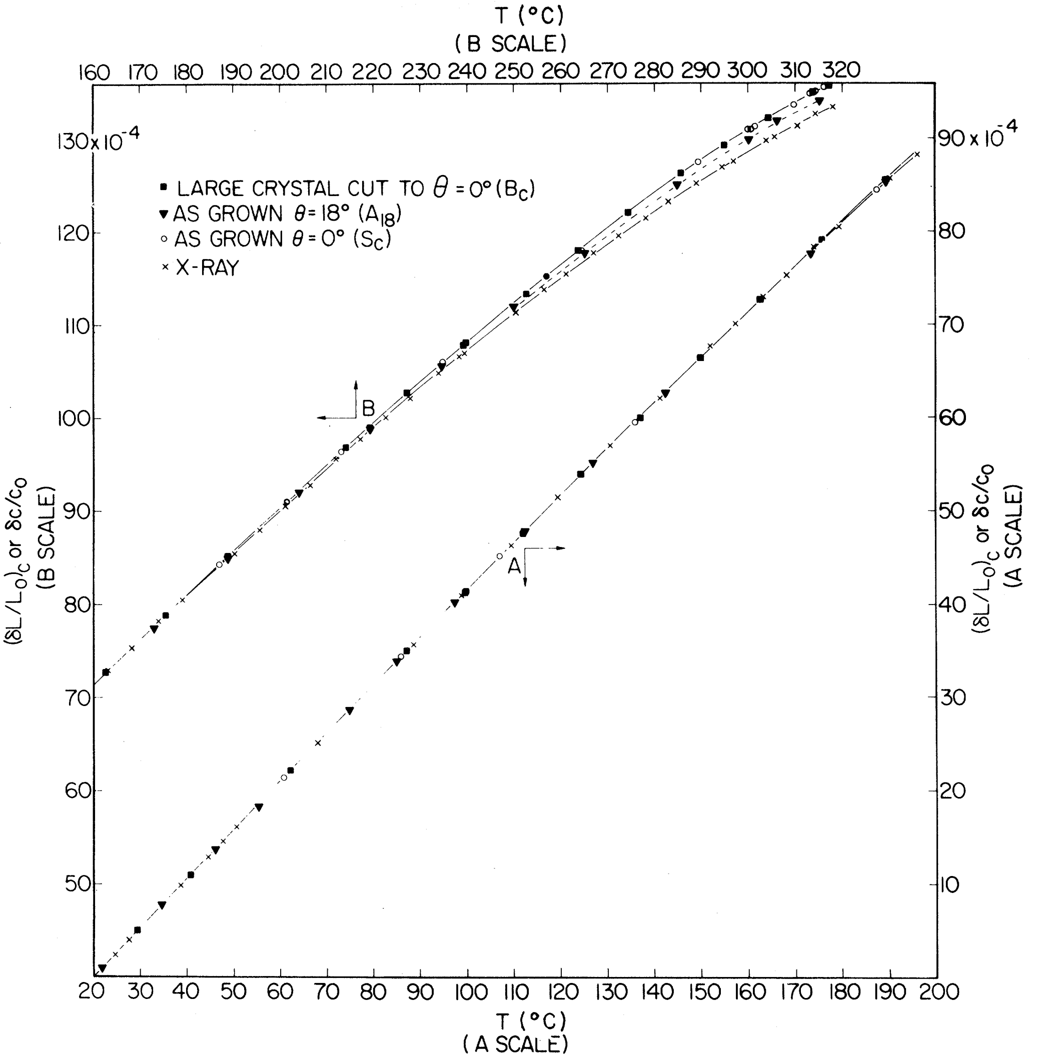

FIG. 1. Comparison of dilatometric $(\delta L/L_0)_c$ and x-ray $(\delta c/c_0)$ thermal expansions parallel to the c axis. Dilatometric measurements were carried out on three samples; the data from two of these (B_c and S_c) coincide while those from the third (A_{18}) fall on the dashed curve. Note the two scales A and B for the different parts of the curve.

$\delta c/c_0$ at regular intervals of temperature, as obtained from the smoothed curves of the x-ray data shown in Figs. 1 and 2. In general, these data are in rough agreement[7] with similar measurements made in the past.[8-10] It is also of interest to combine the data in Tables II and III to obtain, first, the c/a ratio as a function of temperature and second, the change in volume of the unit cell as a function of temperature. The variation of these quantities with temperature is shown in Figs. 3 and 4. It is interesting that the volume expansion follows a curve closer to a straight line than either of the two length expansions.

We turn now to examine the differences between the dilatometric and x-ray data in greater detail. As indicated in the Introduction, the equilibrium vacancy concentration may be obtained from Eq. (1), provided that the data for the differences Δ_c and Δ_a are obtained from the same sample. In the present case, such data are available from the measurements on the samples B_c and B_a, cut from the same large crystal. In order to obtain Δ_c, it is not possible directly to take the difference between $(\delta L/L_0)_c$ and $\delta c/c_0$ at each temperature, since the x-ray data points are not, in general, measured at the same set of temperatures as are

TABLE II. Absolute values of lattice parameters of cadmium at 26 °C.

	Present work	ASTM value
a	(2.97910 ± 0.00009) Å	2.9793 Å
c	(5.61792 ± 0.00012) Å	5.6181 Å

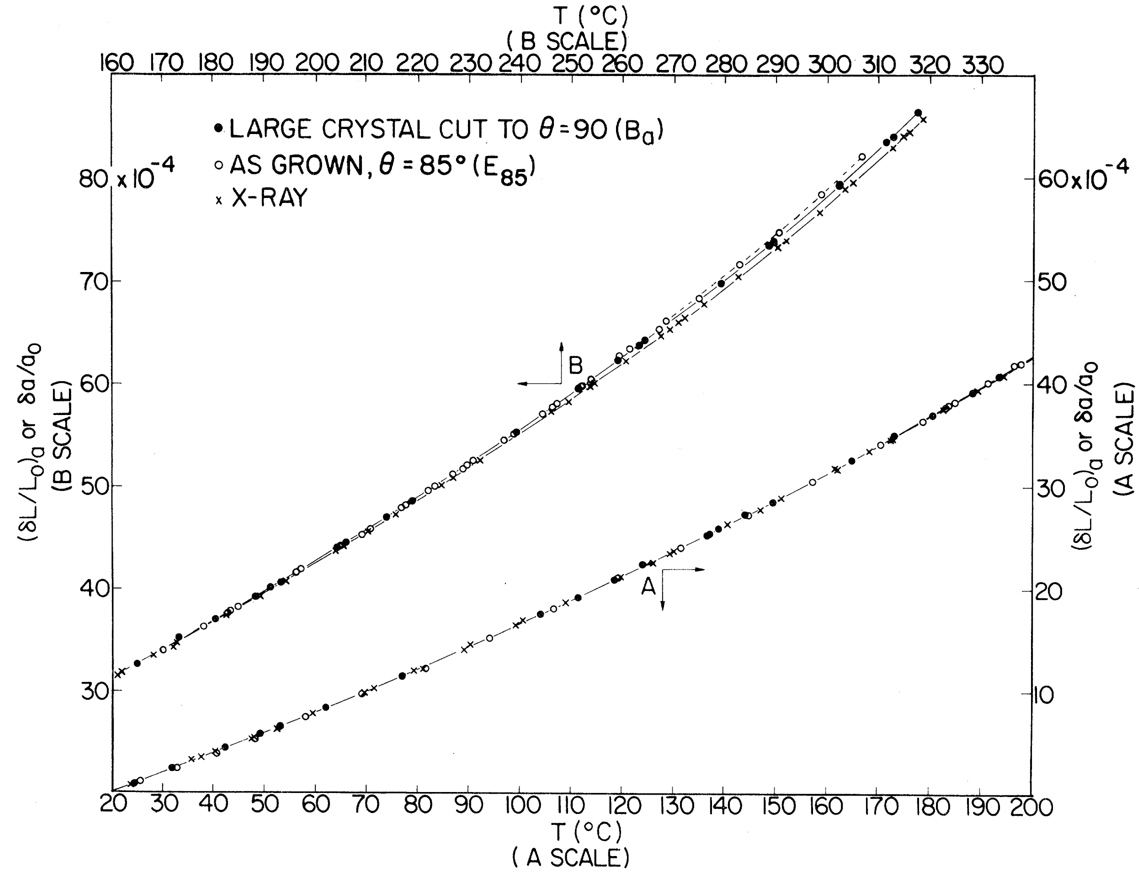

FIG. 2. Comparison of dilatometric and x-ray thermal expansion parallel to the *a* axis. Dilatometric data were obtained from two samples, B_a and E_{85}.

the dilatometric points. In view of the higher precision of the dilatometric data, however, the difference Δ_c was taken between the *smoothed* curve for $(\delta L/L_0)_c$ and the individual experimental points for $\delta c/c_0$, both at the same temperature. The same procedure was also followed for Δ_a. These two difference curves, Δ_c and Δ_a are plotted in Fig. 5 on a semilogarithmic scale vs reciprocal absolute temperature. Finally, the combination $2\Delta_a + \Delta_c$, which should give the vacancy concentration if monovacancies are the dominant defect present, is also plotted vs T^{-1}. The fact that this last plot is a straight line within experimental error, is consistent with the assumption that only monovacancies need be considered. From this plot, we obtain a value of 5.6×10^{-4} for the mole fraction of vacancies at the melting point. In addition, from the slope and intercept of the straight line and utilizing Eqs. (2) and (3), we obtain a value of $H_v^f = (0.40 \pm 0.02)$ eV for the enthalpy of formation and $S_v^f/k = 0.3 \pm 0.4$ for the entropy of formation of a vacancy in cadmium. (The uncertainties quoted represent the two extreme straight lines which can be drawn through the upper curve of Fig. 5 consistent with experimental error.) These results constitute all of the thermodynamic information available from the data.

Values of the ratio Δ_c/Δ_a obtained from the data plotted in Fig. 5 are shown as a function of tem-

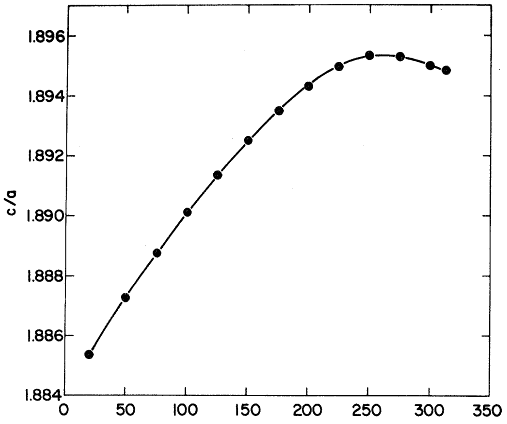

FIG. 3. Variation of the ratio *c/a* with temperature for cadmium metal.

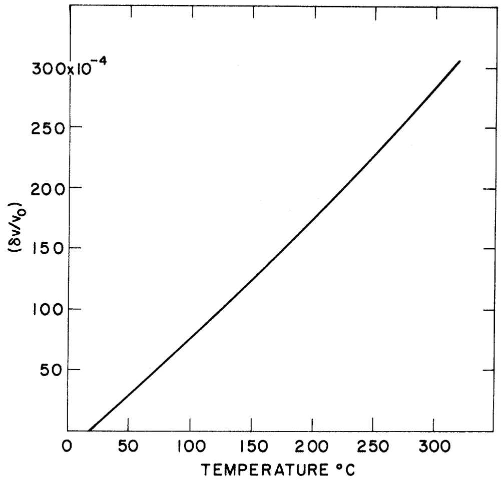

FIG. 4. Fractional change in the volume of the unit cell as a function of temperature for cadmium metal.

perature in Fig. 6. It is clear that, within the experimental scatter, this ratio is nearly independent of the temperature in the range from 180 to 320 °C, with a best value of about 2. 3. This same information is also shown in Fig. 5 by drawing straight lines through the Δ_c and Δ_a curves which are parallel to each other and to the line through the curve of $2\Delta_a + \Delta_c$.

It remains to examine the question of discrepancies in dilatometric data among different samples. Such discrepancies are not unexpected, since it was predicted in paper I that there would be discrepancies in Δ_a and Δ_c due to differences in the dislocation distributions in different crystals. Nevertheless, the fact that samples S_c and B_c, both having $\theta = 0°$ but grown differently (see Table I), gave results for Δ_c which agreed exactly while that for A_{18}, which required correction, did not agree, was a source of concern. It was therefore desirable to check whether the discrepancy lay in the manner of making the correction rather than in a true difference in dislocation structures. Accordingly, another sample B_{18} was cut from the boule such that its angle θ was 18°. The dilatometric data for this sample were then corrected in exactly the same way as that for A_{18}, to obtain $(\delta L/L_0)_c$. The data from B_{18} were not included in Fig. 1 to avoid confusion, but it is shown in Fig. 7. This figure plots Δ_c vs T^{-1} for crystals B_c, B_{18}, and A_{18}. From these results it is clear that the data for the two identically oriented crystals B_{18} and A_{18} are not in agreement. Rather, B_{18} agrees quite closely with the other sample B_c from the same boule (although there is a small but significant disagreement in the two highest-temperature points), while the results for A_{18} fall well below. The question might also arise as to whether we can be sure that both A_{18} and B_{18} have the same θ value to within better than 1°. It should be realized, however, that on this point we are not relying solely on an x-ray orientation determination. Rather, if the θ values were not the same to within at least $\frac{1}{2}°$, there would be a disagreement in the thermal expansion of the two crystals in the range below 165 °C, i. e., below the

TABLE III. Numerical data for $\delta a/a_0$ and $\delta c/c_0$ as a function of temperature.

Temperature (°C)	$\delta a/a_0$ $\times 10^4$	$\delta c/c_0$ $\times 10^4$
20	0	0
40	3.85	10.60
60	7.90	21.02
80	12.11	31.70
100	16.60	41.73
120	21.30	51.80
140	26.15	61.68
160	31.20	71.50
180	36.70	81.00
200	42.42	90.10
220	48.65	99.02
240	55.15	107.42
260	62.00	115.17
280	69.25	122.22
300	77.40	128.50
318	85.50	133.35

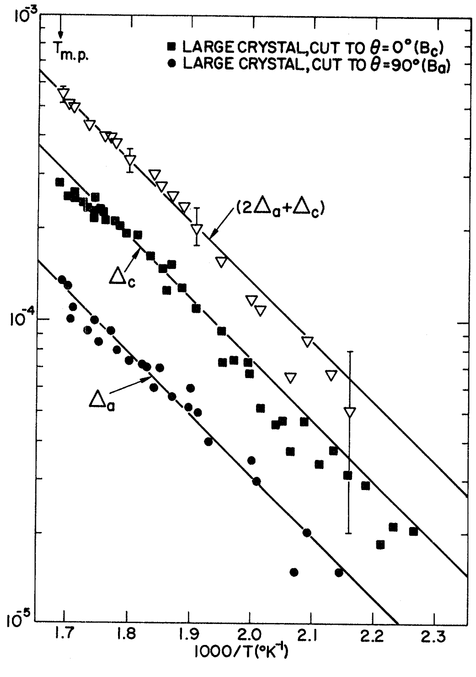

FIG. 5. Variation of the quantities Δ_c, Δ_a, and $2\Delta_a + \Delta_c$ with reciprocal absolute temperature, for dilatometric data obtained from samples cut from the large crystal or boule. Note the vertical error bars.

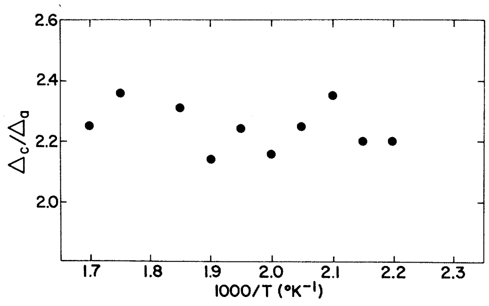

FIG. 6. Variation of Δ_c/Δ_a with reciprocal absolute temperature, from the data in Fig. 5.

range where vacancy formation can be detected. Actually no such disagreement occurs.

Accordingly, it may be concluded that sample A_{18} has a value of $\Delta_c = 1.4\times10^{-4}$ at the melting point, as against a value of $\Delta_c = 3.0\times10^{-4}$ for crystals taken from the boule. Since the quantity $2\Delta_a + \Delta_c$ is a thermodynamic quantity it must be the same for all crystals. We may therefore use the value $2\Delta_a + \Delta_c = 5.6\times10^{-4}$ at 320 °C, together with the above value of Δ_c, to compute the ratio Δ_c/Δ_a for crystal A_{18} near the melting point. In this way, a value $\Delta_c/\Delta_a = 0.7$ is obtained, as against the value 2.3 obtained from samples cut from the boule.

In a similar way, values of Δ_a from crystal B_a cut from the boule and from crystal E_{85} are compared in Fig. 8. Here again there is a real discrepancy, such that Δ_c is 1.6 times higher at the melting point for crystal E_{85} than for B_a. Again, knowing $2\Delta_a + \Delta_c$ and Δ_a, it is possible to compute the ratio Δ_c/Δ_a for crystal E_{85} at 320 °C. The value obtained is 0.8.

Note that in Figs. 5, 7, and 8, all curves have been drawn parallel to each other and with the same slope as that of the thermodynamic data $(2\Delta_a + \Delta_c)$ of Fig. 5. This indicates that the ratio Δ_c/Δ_a for all samples can be taken as independent of temperature to within experimental error, although the possibility for some temperature variation of this ratio is clearly not ruled out.

Gilder and Wallmark[3] have claimed that they could obtain the equivalent of the x-ray data for zinc by extrapolation of dilatometric data from a limited (but apparently arbitrary) temperature range. Since both sets of data are available for cadmium, we have attempted various extrapolations of the dilatometric data from different ranges. We were forced to conclude that there is no rational method of extrapolation which yields the correct x-ray results. It is, therefore, difficult for us to accept any of the vacancy-formation parameters for zinc reported by those authors.

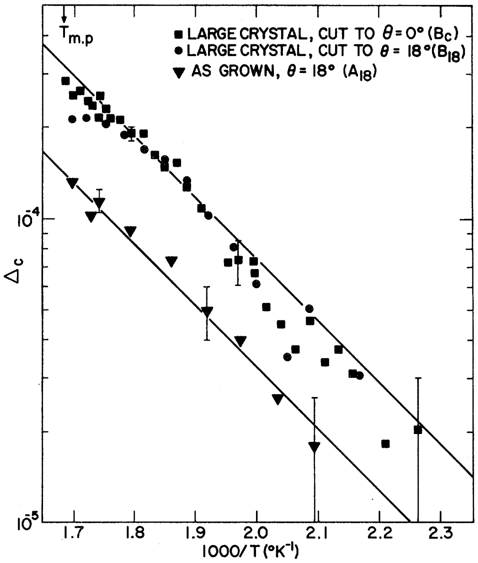

FIG. 7. Comparison of data for Δ_c vs T^{-1} from two samples (B_c and B_{18}) obtained from the large crystal with the corresponding data for a separately grown crystal (A_{18}).

V. DISCUSSION

As already mentioned, the sample dependence for either Δ_c or Δ_a, which was predicted in paper I based on the existence of different dislocation distributions in samples grown differently, has been clearly demonstrated (see Figs. 7 and 8). It therefore follows that, in order to obtain reliable data for the vacancy concentration at elevated temperatures, it is necessary to use differently oriented samples cut from the same crystal. Even when this was done in the present experiments, small discrepancies are found (as in comparing

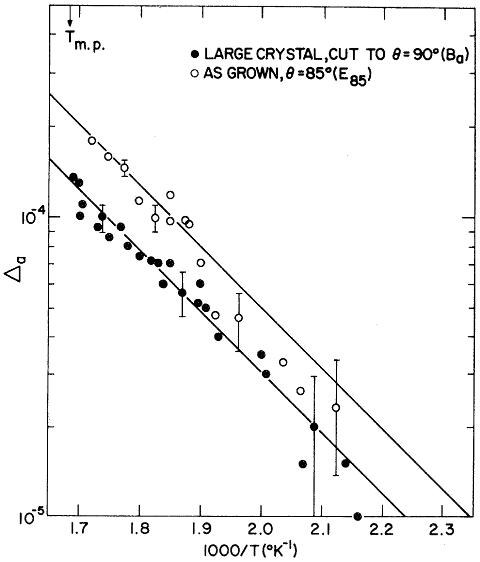

FIG. 8. Comparison of data for Δ_a vs T^{-1} for a sample (B_a) cut from the large crystal with the corresponding data for a separately grown crystal (E_{85}).

the data from B_{18} and B_c in Fig. 7) indicating that the dislocation distribution in different samples cut from the same large crystal is not quite the same. The fact that other workers[3,4] who studied hcp metals used crystals of different orientations which were separately grown, means that the reliability of their results for vacancy concentration may be less than they had anticipated.

A collection of the best data now available for the atomic transport properties in Cd is presented in Table IV, which includes the present results for the vacancy-formation enthalpy and entropy, the activation energies Q and pre-exponential constants D_0 obtained from self-diffusion experiments parallel and perpendicular to the c axis,[11] and additional parameters deduced from these two sets of measurements. As for most of the fcc metals, it again turns out that H_v^f is close to one-half the activation energy for self-diffusion. The activation enthalpy H_v^m for vacancy motion parallel and perpendicular to the c axis are found to be 0.41 and 0.45 eV, respectively. These values are similar to the activation energy in one stage of annealing of cold-worked[12] and neutron-irradiated[13] cadmium.

The low value for the entropy of formation S_v^f of a vacancy in cadmium should be noted. It is interesting that a similar low value, $S_v^f/k \sim 0$ has also been reported by Janot *et al.*[4] for magnesium. It is not yet clear as to why these values in hcp metals should be lower than those in cubic metals (which fall about $S_v^f/k \sim 1.5$). Values of the activation entropy for vacancy motion parallel and perpendicular to the c axis $[(S_v^m)_\parallel$ and $(S_v^m)_\perp$, respectively$]$ are obtained from the two values of D_0 for diffusion, with the aid of the relations[14]

$$D_{0\parallel} = \tfrac{3}{4} c^2 \nu_0 f e^{[S_v^f + (S_v^m)_\parallel]/k}, \tag{6}$$

$$D_{0\perp} \simeq 2 a^2 \nu_0 f e^{[S_v^f + (S_v^m)_\perp]/k}. \tag{7}$$

Here ν_0 is taken as the Debye frequency and f is a correlation factor taken as 0.78. Equation (7) is an approximation, valid when jump frequencies in the basal plane and between basal planes are nearly equal. The activation entropies so obtained are listed in Table IV.

The more unusual matter that the data obtained here permit us to consider is the question of what are the sources and sinks for vacancies as these crystals are heated or cooled at elevated temperatures. In view of the fact that our samples are pure single crystals, we need only consider the external surfaces or the dislocation network (including subboundaries) as possible sources and sinks. If the surfaces were involved, equilibration could only be achieved via diffusion of vacancies through half the thickness of the entire crystal. Since the self-diffusion coefficients are of the order 10^{-8} cm^2/sec near the melting point, and the vacancy-diffusion coefficient $D_v = D/\bar{C}_v \sim 10^{-5}$ cm^2/sec, this would mean that the equilibration time is of the order of 10^4 sec. Experimentally, it was found that equilibration of the length changes in the dilatometer took place just as rapidly as the temperature stabilized itself, i.e., in times of the order of seconds, at most. Thus, diffusion in from the surfaces could only play a negligible role. On the other hand, in terms of a simple model of a regular array of straight parallel dislocations of density Λ, the time constant for equilibration is[15] $\tau \sim (\Lambda D_v)^{-1}$. Our observation that $\tau < 10$ sec is then consistent with this model provided that $\Lambda > 10^4$ cm^{-2} which is quite reasonable for the usual melt-grown crystals.

We turn now to the interpretation of the observed values of the ratio Δ_c/Δ_a in terms of the theory developed in paper I. In that paper, it was shown that the temperature dependence or independence of Δ_c/Δ_a is of some significance. Specifically, for the diffusion-limited case it is expected that Δ_c/Δ_a will be almost temperature independent [paper I, Eq. (25)]. On the other hand, for the climb-rate-limited case one may also obtain temperature independence under suitable assumptions [paper I, Eq. (27)]. Thus, the observed temperature independence of this ratio (Fig. 6) cannot be regarded as conclusively establishing diffusion-limited behavior. By contrast to the present results Janot *et al.*[4] claim a very strong temperature dependence of Δ_c/Δ_a for magnesium.

The absolute value of Δ_c/Δ_a represents a single quantity which gives the relative contribution from dislocations whose unit normal in the slip plane $\vec{n}$ (or components thereof) lie parallel to the c axis to those for which $\vec{n}$ lies in the basal plane. It is a composite quantity, involving summation (or integration) over the entire dislocation distribution

TABLE IV. Summary of parameters related to vacancies and atomic transport in cadmium.

Quantity	Value[a]	Reference
H_v^f (eV)	0.40	This work
$Q_\parallel$ (eV)	0.81	11
$Q_\perp$ (eV)	0.85	11
$(H_v^m)_\parallel$(eV)	0.41	...
$(H_v^m)_\perp$(eV)	0.45	...
S_v^f/k	0.3	This work
$D_{0\parallel}$(cm^2/sec)	0.12	11
$D_{0\perp}$(cm^2/sec)	0.18	11
$S_v^m)_\parallel/k$	2.4	...
$(S_{v\perp}^m/k$	3.1	...

[a] The uncertainty in the diffusion-activation energies is ~ ±0.01 eV while that of H_v^f from the present work is ±0.02 eV. The uncertainty in the deduced quantities S_v^m/k is ~ ±0.4.

in accordance with Eqs. (17) or (25) of paper I. To interpret this quantity, it is helpful to know in some detail what is the dislocation distribution in the sample under consideration. Unfortunately, there have been few observations of the dislocation structure in well-annealed bulk cadmium crystals (or in the, presumably similar, metal zinc) using x-ray topography.[16,17] The most important slip system is of course, the $\langle 11\bar{2}0\rangle\{0001\}$, i.e., involving dislocations which lie in the basal plane and have Burgers vector equal to the nearest-neighbor spacing $\vec{a}$. Such dislocations have their unit normal vectors $\vec{n}$ in the basal plane, and their climb therefore contributes only to Δ_a. If only such basal dislocations were present, Δ_c would be zero. We must conclude, therefore, that in the present large crystal or boule, for which $\Delta_c/\Delta_a = 2.3$, the major contribution of vacancies comes from the climb of nonbasal dislocations. (Even in crystals A_{18} and E_{85} for which we have estimated a ratio of 0.7–0.8, an appreciable contribution must come from nonbasal dislocations.) The reason may be related not so much to the existence of a high density of nonbasal dislocations as to the fact that basal dislocations in Cd may climb at very low efficiency. This inefficiency can be due to the relatively low stacking-fault energy[18] and, therefore, to the ease of dissociation of basal-plane dislocations into partials separated by a relatively wide stacking fault. In such a case, in order for climb to take place, the two partials must first come together, a process which may require a high activation energy.[19]

Accordingly, we turn our attention to nonbasal dislocations in cadmium. Contributions to Δ_c can be obtained from dislocations which have Burgers vector $\vec{b} = \vec{a} = \frac{1}{3}\langle 11\bar{2}0\rangle$, provided that the dislocation line does not lie in the basal plane and also is not of edge type (since then, $\vec{n} = \vec{b}$). On the other hand, when such dislocations are averaged over all orientations, the contribution to Δ_a will be much greater than to Δ_c. Of greater interest, therefore, are dislocations whose Burgers vectors do not lie in the basal plane. The next simplest case is that for which $\vec{b} = \vec{c} = [0001]$; such dislocations have been observed in Cd.[17] An edge dislocation with this Burgers vector clearly contributes only to Δ_c. On the other hand nonedge dislocations with this Burgers vector contribute both to Δ_c and Δ_a, and taking a random distribution of orientations of such dislocations in the diffusion-limited approximation, we obtain $\Delta_c/\Delta_a = 4$ (see Appendix A).

The work of Price[18] shows that nonbasal glide occurs especially via dislocations whose Burgers vector is of the type $\vec{c} + \vec{a} = \frac{1}{3}\langle 11\bar{2}3\rangle$. Dislocations having this Burgers vector have also been observed in annealed Cd.[17] Edge dislocations of this type, when present alone, contribute $\Delta_c/\Delta_a = 2\cot^2\psi = 2c^2/a^2 = 7.1$ [see paper I, Eq. (23)]. On the other hand, allowing for the presence of other than edge orientations will serve to bring down this ratio. Thus, for example, when dislocations with this Burgers vector are randomly distributed on pyrimidal planes of the type $\{11\bar{2}2\}$ a value $\Delta_c/\Delta_a = 1.3$ is obtained (see Appendix B). Similar results for other planes are also given.

The various possibilities quoted here only serve to show that, by considering nonbasal dislocations, the occurrence of relatively large values for the ratio Δ_c/Δ_a may be understood. Realizing that efficiency of climb motion is not related to efficiency of glide motion, there is no reason to expect a predominance of basal-plane dislocations in climb. In fact, as already mentioned, due to the splitting of basal dislocations into partials, they may in fact be relatively ineffective in the climb process. The weakness of the present type of experiment is that it determines a single number representing the climb contribution of the entire assembly of dislocations in the crystal. Clearly, more effective use of this experiment can be made when a controlled distribution of dislocations is introduced into the sample, or when it is accompanied by direct observation of the dislocation structure via x-ray topographic methods.

ACKNOWLEDGMENTS

The authors are grateful to H. P. Charbnau for valuable assistance in sample preparation and data reduction, and to J. J. Burton for helpful comments on the manuscript.

APPENDIX A: CALCULATION OF Δ_c/Δ_a FOR A RANDOM DISTRIBUTION OF DISLOCATIONS WITH $\vec{b} = [0001]$

Assume that the dislocation lines lie at random orientations to the c axis. This means that the probability that the normal $\vec{n}$ lies at angle ψ to the c axis is $\propto \cos\psi$, or

$$\frac{d\Lambda}{d\psi} = \Lambda_t \cos\psi \; , \tag{A1}$$

where Λ_t is the total dislocation density. From Eq. (25) of paper I, representing the diffusion limited approximation, we obtain, after converting the sum to an integral,

$$\frac{\Delta_c}{\Delta_a} \equiv \frac{2\int_0^{\pi/2} \cos^3\psi \, d\psi}{\int_0^{\pi/2} \cos\psi \sin^2\psi \, d\psi} = 4. \tag{A2}$$

APPENDIX B: CALCULATION OF Δ_c/Δ_a FOR A RANDOM DISTRIBUTION OF DISLOCATIONS ON A PLANE

It is desirable to obtain the formula for the ratio Δ_c/Δ_a for a collection of dislocations randomly distributed on a given type of slip plane, of indices $\{hkil\}$. Since the dislocation lines are taken as random in the plane, the normals $\vec{n}$ are also ran-

TABLE V. Results of Eq. (B3) for three planes in the hcp structure which contain a Burgers vector of the type $\vec{c}+\vec{a}$.

Plane	$\cos^2\psi_0$	Δ_c/Δ_a
$\{01\bar{1}0\}$	1	2
$\{11\bar{2}2\}$	$\frac{c^2}{c^2+a^2}=0.78$	1.3
$\{10\bar{1}1\}$	$\frac{c^2}{c^2+a^2(3/4)}=0.83$	1.4

dom, so that

$$\frac{d\Lambda}{d\phi}=\frac{\Lambda_t}{2\pi}\ , \tag{B1}$$

where ϕ is the angle between $\vec{n}$ and the projection of the c axis into the plane and Λ_t is the total dislocation density. Further, if ψ_0 is the angle between the c axis and its projection in the plane, then the angle ψ between $\vec{n}$ and the c axis is given by

$$\cos\psi=\cos\psi_0\cos\phi\ . \tag{B2}$$

Thus, from Eq. (25) of paper I, with the sums converted into integrals,

$$\frac{\Delta_c}{\Delta_a}=2\,\frac{\int d\Lambda\cos^2\psi}{\int d\Lambda\sin^2\psi}=\frac{\cos^2\psi_0}{1-\frac{1}{2}\cos^2\psi_0}\ , \tag{B3}$$

where we have substituted for $d\Lambda$, Eq. (B1) with

$$d\phi=\frac{\sin\psi\,d\psi}{[\cos^2\psi_0-\cos^2\psi]^{1/2}}$$

obtained from Eq. (B2), and then evaluated the resulting integrals between the limits $\psi=\psi_0$ to $\frac{1}{2}\pi$.

Note that for $\psi_0=0$, i.e., for a plane containing the c axis, Eq. (B3) gives $\Delta_c/\Delta_a=2$, while for the basal plane ($\psi_0=\frac{1}{2}\pi$), $\Delta_c/\Delta_a=0$. Table V lists the results of Eq. (B3) for three of the important types of planes of the hcp structure, all of which contain the Burgers vector of type $\vec{c}+\vec{a}$.

---

†Work supported in part by the U.S. Atomic Energy Commission.

[1] A. S. Nowick and R. Feder, preceding paper, Phys. Rev. B 5, 1238 (1972), hereafter referred to as paper I.

[2] See Refs. 2–7 in paper I.

[3] H. M. Gilder and G. N. Wallmark, Phys. Rev. 182, 771 (1969).

[4] C. Janot, D. Mallējac, and B. George, Phys. Rev. B 2, 3088 (1970).

[5] R. Feder and H. P. Charbnau, Phys. Rev. 149, 464 (1966).

[6] ASTM x-ray-powder-data file.

[7] The data obtained by previous workers are not in close agreement with each other. They fall, about equally, both above and below the present results.

[8] G. F. Kossolapow and A. K. Trapensikow, Z. Krist. 91, 410 (1935)

[9] E. A. Owen and E. W. Roberts, Phil. Mag. 22, 290 (1936).

[10] D. A. Edwards, W. E. Wallace, and R. S. Craig, J. Am. Chem. Soc. 74, 5256 (1952).

[11] E. S. Wajda, G. A. Shirn, and H. B. Huntington, Acta Met. 3, 39 (1955); C. W. Mao (private communication).

[12] H. R. Peiffer and F. R. Stevenson, J. Appl. Phys. 34, 2804 (1963).

[13] R. R. Coltman, C. E. Klabunde, J. K. Redman, and A. L. Southern, Rad. Effects 7, 235 (1971).

[14] J. G. Mullen, Phys. Rev. 124, 1723 (1961).

[15] A. C. Damask and G. J. Dienes, *Point Defects in Metals* (Gordon and Breach, New York, 1963), Chap. 2.

[16] J. M. Schultz and R. W. Armstrong, Phil. Mag. 10, 497 (1964).

[17] A. S. T. Badrick, thesis (University of Surrey, 1969) (unpublished).

[18] P. B. Price, in *Electron Microscopy and the Strength of Crystals*, edited by G. Thomas and J. Washburn (Wiley, New York, 1963).

[19] J. P. Hirth and J. Lothe, *Theory of Dislocations* (McGraw-Hill, New York, 1968), Sec. 15-6.